Effect of the Schottky barrier height on the detection of midgap levels in 4*H*-SiC by deep level transient spectroscopy

S. A. Reshanov[a)] and G. Pensl
Institute of Condensed Matter Physics, University of Erlangen-Nürnberg, Staudtstrasse 7,
91058 Erlangen, Germany

K. Danno and T. Kimoto
Department of Electronic Science and Engineering, Kyoto University, Katsura, Nishikyo,
Kyoto 615-8510, Japan

S. Hishiki, T. Ohshima, and H. Itoh
Japan Atomic Energy Agency, 1233 Watanuki, Takasaki, Gunma 370-1292, Japan

Fei Yan, R. P. Devaty, and W. J. Choyke
Department of Physics, University of Pittsburgh, Pittsburgh, Pennsylvania 15260, USA

The effect of the Schottky barrier height on the detection of the concentration of midgap defects using deep level transient spectroscopy (DLTS) is experimentally and theoretically studied for EH_6 and EH_7 defects in 4*H*-SiC. In this special case, the DLTS signal height for EH_6 and EH_7 increases with increasing barrier height and saturates at values above 1.5 and 1.7 eV, respectively. Below 1.1 eV, the DLTS peak completely disappears for both defects. The experimental data are explained by a theoretical model. The course of the quasi-Fermi level in the space charge region is calculated as a function of the reverse current through it, which is determined by the barrier height, and the reverse bias applied. © *2007 American Institute of Physics*. [DOI: 10.1063/1.2818050]

I. INTRODUCTION

Midgap levels in a semiconductor are predominantly responsible for the limitation of the lifetime of free minority carriers and consequently for the degradation of the performance of bipolar electronic devices. Such defects can be detected by deep level transient spectroscopy (DLTS). Ma *et al.*[1] demonstrated in GaAs that the observed concentration of the energetically deep EL2 defect is extremely sensitive to the Schottky barrier height used for the DLTS measurement.

In high-quality 4*H*-SiC epilayers, the EH_6/EH_7 centers are the dominating midgap defects.[2] They exist in as-grown material and can in addition be generated by electron irradiation or implantation of ions. The EH_6/EH_7 centers were intensively studied with DLTS using Ni Schottky contacts.[2–5] On the other hand, these centers could not be observed when Ti/Al Schottky contacts were used.[6]

In this paper, we conduct systematic DLTS investigations in 4*H*-SiC with regard to the detection of the midgap defects EH_6 ($E_{EH_6}=E_C-1.39$ eV, $\sigma=6\times10^{-14}$ cm^2) and EH_7 ($E_{EH_7}=E_C-1.53$ eV, $\sigma=7\times10^{-14}$ cm^2) by using different metals for the Schottky contact. Further we explain the experimental data on the basis of the diffusion and thermionic theory,[7] which determine the current through the Schottky barrier at reverse bias.

II. EXPERIMENTAL DETAILS

We used square-shaped (4×4 mm^2) samples cut from an *n*-type 4*H*-SiC wafer with an *n*-type epilayer containing a nitrogen donor concentration of $[N]=2.8\times10^{15}$ cm^{-3}. The midgap defects were generated by electron irradiation [$E(e)=170$ keV, fluence $D=5\times10^{16}$ cm^{-2}]. The investigated samples were annealed either at 1000 °C (sample 1) or at 1100 °C (sample 2) for 30 min. For the capacitance-voltage (*C-V*) and DLTS measurements, we deposited first Ni Schottky contacts through a shadow mask (diameter of the circular spot=1.0 mm) and performed then the electrical measurements. Finally, we removed the Ni contacts, performed a RCA cleaning of the surface, and deposited another metal on the same sample. In sequence, we used Ni, Pd, Au, Ir, and W. The DLTS measurements were examined on two samples and on a series of different contacts of each sample. In all the cases, the defect concentrations obtained were reproducible.

The Schottky barriers for the different metals were determined by *C-V* measurements (probe frequency $\omega=1$ MHz). The *C-V* measurements were performed at room temperature before and after the DLTS measurements and at $T=690$ K, which is the temperature where the DLTS peak maxima appear (see Table I). The barrier height Φ_b changes with the temperature for several reasons. With increasing temperature, a reversible decrease of Φ_b is observed due to the band gap narrowing and an irreversible change is connected due to the chemical interaction of the metal with SiC. This chemical interaction is especially observed for Ni and Ir, which typically form silicides at the interface. For the evaluation, we used the barrier height values determined at the temperature, where the EH_7 peak was observed in the DLTS spectra. Depending on the particular preparation of the SiC surface, the Schottky barrier heights differ slightly; they

a)Electronic mail: sergey.reshanov@physik.uni-erlangen.de

TABLE I. Diffusion voltage U_i and barrier height Φ_b of Schottky contacts prepared on *n*-type 4*H*-SiC samples 1/2. The barrier height is determined by C–V measurements at 300 K before and after the DLTS scan as well as at 690 K (subsequent to the measurements at 300 K).

Metal	$T=300$ K (before DLTS)		$T=690$ K		$T=300$ K (after DLTS)	
	U_i (V)	Φ_b (eV)	U_i (V)	Φ_b (eV)	U_i (V)	Φ_b (eV)
Ni	1.59/1.55	1.81/1.77	1.24/1.20	1.83/1.79	1.77/1.66	1.99/1.89
Pd	1.59/1.50	1.82/1.72	1.06/0.97	1.65/1.56	1.56/1.48	1.78/1.70
Au	1.31/1.29	1.54/1.52	0.83/0.83	1.42/1.42	1.37/1.33	1.60/1.56
Ir	1.26/1.23	1.49/1.45	0.80/0.78	1.40/1.38	1.41/1.35	1.63/1.57
W	1.01/0.94	1.23/1.17	0.55/0.49	1.14/1.08	1.05/1.00	1.27/1.22

resulted in Φ_b(Ni)$=1.79$–1.83 eV, Φ_b(Pd)$=1.56$–1.65 eV, Φ_b(Au)$=1.42$ eV, Φ_b(Ir)$=1.38$–1.40 eV, and Φ_b(W) $=1.08$–1.14 eV.

Figure 1 shows DLTS spectra taken on the same sample with a reverse bias $U_R=-4$ V but using different metal/4*H*-SiC Schottky contacts. It turns out that the DLTS peak height of the EH_6 and EH_7 defects—and as a consequence, the observed defect concentration—distinctly increases with the barrier height, while the peak height of the energetically shallower Z_1/Z_2 defect is constant for all the metals employed. In the case of the EH_6/EH_7 defect, the striking feature, however, is that an increase of the potential barrier between the semiconductor and the Au contact by changing the external reverse bias from -4 to -4.4 V, which theoretically corresponds to the Ni/4*H*-SiC potential barrier at -4 V, does not drastically increase the EH_6/EH_7-peak height as shown in Fig. 2. The concentrations of the EH_6 and EH_7 defects in Fig. 3 are normalized by the corresponding concentrations obtained from Ni/4*H*-SiC Schottky contacts and are plotted as a function of the barrier height Φ_b used for the DLTS measurement. For $\Phi_b \geqslant 1.5$ eV and $\Phi_b \geqslant 1.7$ eV, the defect concentrations of the EH_6 and EH_7 centers, respectively, are saturated. For $\Phi_b \leqslant 1.1$ eV, both defects can no longer be observed by DLTS.

III. THEORETICAL MODEL AND DISCUSSION

In order to explain the dependence of the observed DLTS peak heights on the size of the Schottky barrier, we propose and discuss a model that provides the course of the quasi-Fermi level in the space charge region as a function of the current through the depletion region, whereas this current is determined by the barrier height and by the reverse bias applied.

For simplicity, we will use the depletion approximation of a Schottky barrier. In this approximation, the free-carrier density is assumed to be abruptly cut off at the edge of the space charge region. Then, the energy of the conduction band edge relative to the position of the Fermi level in the metal is given by[7]

$$E_C(x) = \Phi_b + \frac{q^2 N_d}{2\varepsilon\varepsilon_0}(x^2 - 2wx). \qquad (1)$$

The width of the depletion layer w is given by $w = \sqrt{2\varepsilon\varepsilon_0 U_d/qN_d}$, where $qU_d = \Phi_b - kT \ln(N_C/N_d) - qU$ is the band bending for the applied bias U. N_C is the effective density of states in the conduction band. For 4*H*-SiC, N_C is equal to $3.26 \times 10^{15} T^{3/2}$ cm^{-3} using the effective conduction band masses $m_{M-\Gamma}=0.58m_0$, $m_{M-K}=0.28m_0$, and $m_{M-L}=0.31m_0$.[8]

The barrier height Φ_b can be extracted from C-V measurements according to $\Phi_b = qU_i + kT \ln(N_C/N_d)$, where the diffusion potential U_i is determined as the intersection point of the x axis with the $1/C^2$ curve as shown in Fig. 4. As an example, the experimental $1/C^2$-U curves for Ni and Ir Schottky contacts are shown in this figure (see full circles and open triangles). These curves are straight lines and pos-
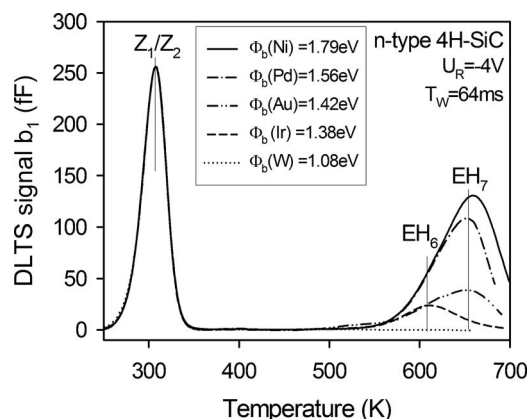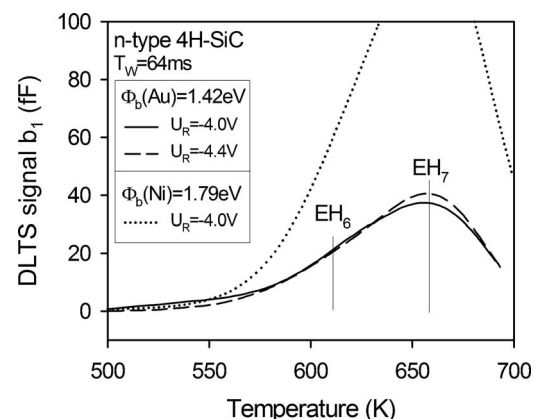

FIG. 1. DLTS spectra taken on the same sample 2 (electron irradiated and annealed at 1100 °C) with constant reverse bias $U_R=-4$ V but with different metal/4*H*-SiC Schottky barriers: Ni (—), Pd (-·-·-·-), Au (-··-··-··-), Ir (----), and W (···-···-).

FIG. 2. DLTS spectra taken on the same 4*H*-SiC sample 2 with a Au Schottky barrier at reverse biases $U_R=-4$ V (solid curve) and $U_R=-4.4$ V (dashed curve), respectively, and for comparison with a Ni Schottky barrier at reverse bias $U_R=-4$ V (dotted curve).
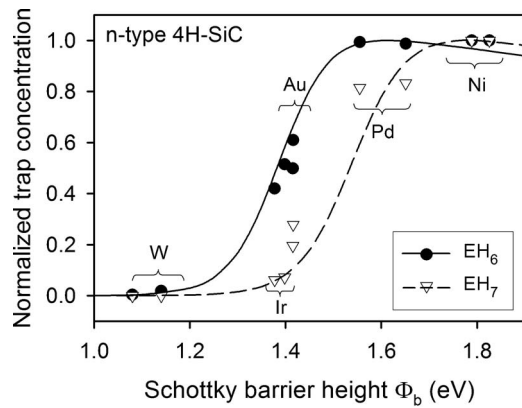
FIG. 3. Normalized trap concentration of the EH_6 and EH_7 defects (as related to the defect concentration obtained from Ni/4H-SiC Schottky contacts) as a function of the Schottky barrier height. The symbols (full circles, open triangles) are experimental data; the solid and dashed curves are theoretically calculated with Eq. (8) without using any fit parameter.

sess identical slopes meaning that the epilayer is homogeneously doped with N donors and that no insulating layer does exist at the metal/SiC interface. The observed shift in the diffusion potential is caused purely by the difference in the barrier height. The intersection points with the x axis result in Schottky barriers of 1.79 and 1.38 eV for the Ni and Ir Schottky contacts, respectively.

The quasi-Fermi level for electrons E_{Fn} is defined by[7]

$$n = N_C \exp[-(E_C - E_{Fn})/kT]. \tag{2}$$

The basic assumption is that the current through the space charge region is only caused by drift and diffusion. Hereby we neglect tunneling through the barrier, the influence of image forces, and the generation/recombination current. Making use of the Einstein relationship, the current density is then given by

$$J = \mu_n n(x)\frac{dE_{Fn}(x)}{dx}, \tag{3}$$

where μ_n is the electron mobility. In high-quality n-type 4H-SiC, the electron mobility for the $\langle 0001 \rangle$ direction can be
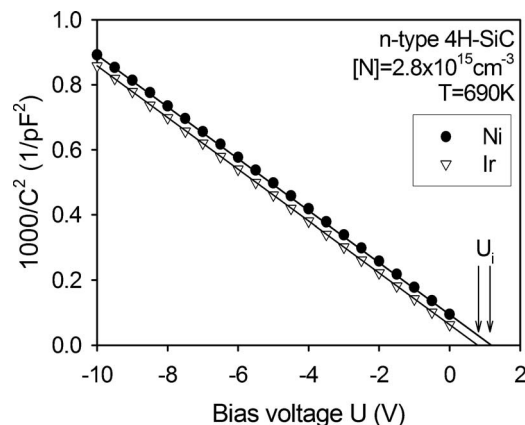

FIG. 4. *C-V* characteristics obtained from Ni and Ir Schottky contacts. The diffusion potential U_i is given by the intercept determined by the intersection point between the linear extrapolation of $1/C^2$ vs U and the x axis.

approximated by $\mu_n(T)=950(300/T)^{2.8}$ cm^2/V s.[9] Inserting Eq. (2) into Eq. (3), we obtain

$$J = kT\mu_n N_C \exp(-E_C/kT)\frac{d}{dx}[\exp(E_{Fn}/kT)]. \tag{4}$$

Integration of Eq. (4) over $0 \leq x \leq w$ results in the course of the quasi-Fermi level in the space charge region,

$$E_{Fn}(x) = kT \ln\left[\exp\frac{E_{Fn}(w)}{kT} - \frac{J}{\mu_n N_C kT}\int_x^w \exp\left(\frac{E_C(x)}{kT}\right)dx\right]. \tag{5}$$

The current under reverse bias $U \ll 0$ is determined by the saturation current,[7]

$$J = A^*T^2 \exp\left(\frac{-\Phi_b}{kT}\right)\left(\exp\frac{qU}{kT} - 1\right)$$
$$\cong -A^*T^2 \exp\left(\frac{-\Phi_b}{kT}\right), \tag{6}$$

where $A^*=4\pi q m_\sigma^* k^2 h^{-3}$ is the effective Richardson constant and m_σ^* is the effective mass of the conductivity of electrons.[10] The effective mass of the conductivity of electrons in the $\langle 0001 \rangle$ direction is composed of the effective electron masses according to $m_{\sigma\langle 0001\rangle}^* = 3(m_{M-\Gamma}m_{M-K})^{1/2}$. For n-type 4H-SiC, the Richardson constant in $\langle 0001 \rangle$ direction results in $A^*=146$ A cm^{-2} K^{-2}.

The measured reverse current density versus barrier height taken at temperatures of 610 and 660 K, where the EH_6 and EH_7 centers appear in the DLTS spectra, are plotted in Fig. 5 (see open triangles and full circles). The current densities calculated with Eq. (6) (see dashed and solid lines in Fig. 5) agree sufficiently well with the experimental data and can therefore be used for the calculation of the quasi-Fermi level in the depletion region.

The course of the quasi-Fermi energy under reverse bias calculated with Eq. (5) for three barrier heights of 1.0, 1.5, and 2 eV using the same band bending of $U_d=5$ V is plotted in Fig. 6 (see dotted curves). For convenience, the energies are related to the Fermi level in the bulk of 4H-SiC. In the case of $\Phi_b=1$ eV, the energy level E_{EH_7} is completely below
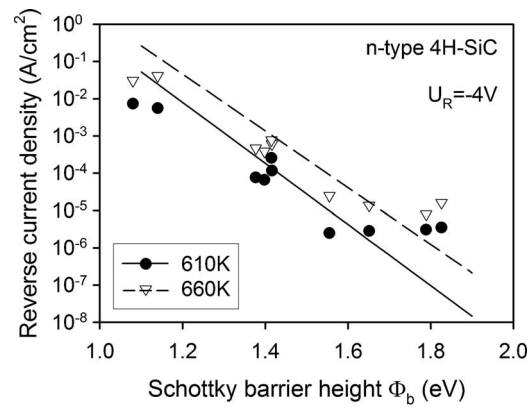

FIG. 5. The reverse current density measured at 610 and 660 K for various Schottky barriers. The solid and dashed lines are calculated with Eq. (6).
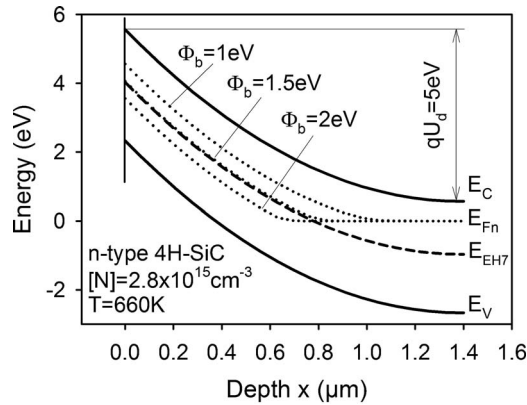
FIG. 6. Band diagram of a Schottky barrier prepared on 4*H*-SiC. The dashed curve corresponds to the level EH$_7$; the dotted curves correspond to the quasi-Fermi level calculated for three different Schottky barrier heights (Φ_b=1, 1.5, and 2 eV) using the same band bending of qU_d=5 eV. The energies are plotted relative to the Fermi level in the bulk of 4*H*-SiC.
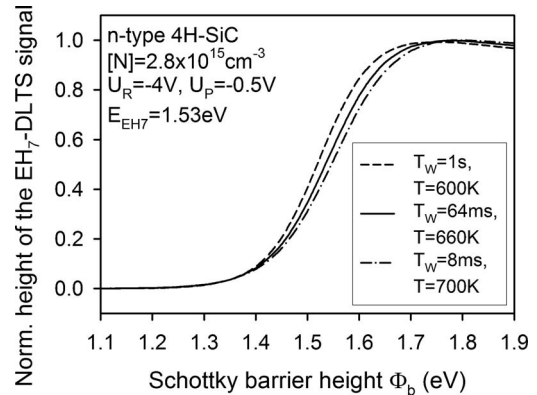

FIG. 7. Normalized DLTS signal of the EH$_7$ defect vs Schottky barrier height for different transient time windows T_W corresponding to different temperature positions T of the peak maxima. The curves are calculated with Eq. (8).

the quasi-Fermi level E_{Fn} in the depletion region and the charge state of this level cannot be changed by applying filling pulses. As a consequence, no electrons can be emitted into the conduction band and therefore no DLTS peak is observed. In the case of Φ_b=2 eV, the EH$_7$ level crosses the quasi-Fermi level. Depending on the strength of the filling pulse, filled traps located in a small zone of the space charge region move above the quasi-Fermi level and contribute to the DLTS signal. This zone is defined by the intersection points between the defect and quasi-Fermi level with and without filling pulse condition. The quasi-Fermi level E_{Fn} for Φ_b=1.5 eV runs largely parallel to the defect level in the depletion region and, depending on the degree of occupation, only a fraction of the deep defects can contribute to the DLTS signal.

In general, as long as the defect level is located above the quasi-Fermi level during reverse bias, empty traps can be filled with electrons by the filling pulse. These electrons are emitted during the DLTS transient and contribute to the DLTS peak. As soon as the defect level is located below the quasi-Fermi level under reverse bias, no additional traps can be filled during the filling pulse and no electrons can be emitted during the DLTS transient. The probability that a trap state E_T is occupied with an electron is given by the Fermi-Dirac function

$$P = \{1 + \exp[(E_T - E_{Fn})/kT]\}^{-1}. \tag{7}$$

The DLTS signal is proportional to the number of trap states, which are occupied with an electron by the filling pulse U_P,

$$S \propto \int_0^w [P(U_P) - P(U_R)]dx. \tag{8}$$

The normalized defect concentrations of EH$_6$ and EH$_7$ are calculated with Eq. (8) as a function of the Schottky barrier height taking into account the course of the quasi-Fermi level in the space charge region [Eqs. (5) and (6)]. The result is plotted in Fig. 3 (see solid and dashed curves). The calculated normalized concentrations of EH$_6$ and EH$_7$ centers as a

function of the Schottky barrier height are in excellent agreement with the experimental data without using any fit parameter.

In Fig. 7, it is demonstrated that the temperature position of EH$_7$ peak maxima has only a minor effect on the normalized EH$_7$-defect concentration. By changing the transient time window T_W from 1 s to 8 ms, the temperature position of the EH$_7$-peak maximum can be shifted from 600 to 700 K. The dashed and dash-dotted curves in Fig. 7 calculated with Eq. (8) show that a marginal variation of the normalized EH$_7$ concentration occurs for 1.4 eV$<\Phi_b$ $<$ 1.7 eV.

IV. CONCLUSION

The position of the quasi-Fermi level in the space charge region, which is determined by the current through the depletion layer, strongly affects the detection of the concentration of energetically deep defects by DLTS. Experimentally this reverse current is dominated by the height of the Schottky barrier. We have demonstrated the dependence of the defect concentration determined by DLTS on the Schottky barrier height for the midgap levels EH$_6$ and EH$_7$ in 4*H*-SiC.

We developed a model that takes into account the facts mentioned above. The current through the Schottky barrier is calculated on the basis of the diffusion and thermionic theory. In Fig. 5, it is shown that this current largely agrees with the measured current. At small and large barrier heights, slight deviations between the theoretical curves and the measurement points are observed, which may be due to the simplifications of our model. We have neglected, e.g., tunneling through the barrier and generation/recombination currents caused by defect levels. Our theoretical analysis determines the course of the quasi-Fermi level in the space charge region as a function of the barrier height and of the reverse bias applied. In the case that the defect level crosses the quasi-Fermi level, additional traps can be filled with electrons when a filling pulse is applied. These traps are emptied again when the filling pulse is switched off, which leads to a measurable DLTS transient. In the case that no intersection point between the defect and quasi-Fermi level does exist, no additional traps can be filled by reducing the reverse bias and

as a consequence no energetically deep defects can be observed. The perfect agreement between our theoretical model and the experimental data in Fig. 3 unambiguously confirms our model. The use of small Schottky barrier heights for DLTS investigations in connection with wide band gap semiconductors may therefore lead to incorrect results with regard to concentrations of energetically deep defects. The Schottky barrier height should be at least of the same size as the activation energy of the defect under investigation. For 4*H*-SiC, Pd may be an alternative for Ni when chemical reactions at the interface have to be avoided. Unlike Ir, W or Ti/Al Schottky contacts are not suitable to study midgap defects in *n*-type 4*H*-SiC.

ACKNOWLEDGMENTS

[1] Q. Y. Ma, M. T. Schmidt, X. Wu, H. L. Evans, and E. S. Yang, J. Appl. Phys. **64**, 2469 (1988).
[2] C. Hemmingsson, N. T. Son, O. Kordina, J. P. Bergman, E. Janzén, J. L. Lindström, S. Savage, and N. Nordell, J. Appl. Phys. **81**, 6155 (1997).
[3] L. Storasta, J. P. Bergman, E. Janzén, A. Henry, and J. Lu, J. Appl. Phys. **96**, 4909 (2004).
[4] K. Danno, T. Kimoto, and H. Matsunami, Appl. Phys. Lett. **86**, 122104 (2005).
[5] G. Alfieri, E. V. Monakhov, B. G. Svensson, and M. K. Linnarsson, J. Appl. Phys. **98**, 043518 (2005).
[6] F. Schmid, S. A. Reshanov, H. B. Weber, G. Pensl, M. Bockstedte, A. Mattausch, O. Pankratov, T. Ohshima, and H. Itoh, Phys. Rev. B **74**, 245212 (2006).
[7] E. H. Rhoderick, J. Phys. D **5**, 1920 (1972).
[8] C. Persson and U. Lindefelt, Phys. Rev. B **54**, 10257 (1996).
[9] D. Stephani and P. Friedrichs, Int. J. High Speed Electron. Syst. **16**, 825 (2006).
[10] C. R. Crowell, Solid-State Electron. **8**, 395 (1965).